Chapter 16
Frequency Determination Using the Discrete Hermite Transform

Dale H. Mugler and Stuart Clary

Abstract This chapter introduces a new method for frequency determination that employs the authors' discrete Hermite transform. Particularly for an input signal that is a linear combination of general sinusoids, this method provides highly accurate estimations of both frequencies and amplitudes of those sinusoids. The method is based primarily on the property of the discrete Hermite functions (DHf) being eigenvectors of the centered Fourier matrix, analogous to the classical result that the continuous Hermite functions (CHf) are eigenfunctions of the Fourier transform. Using this method for frequency determination, a new Hermite transform-based time-frequency representation, the HDgram, is developed that can provide clearer interpretations of frequency and amplitude content of a signal than corresponding spectrograms or scalograms.

16.1 Introduction

For finite-length discrete signals (hereafter referred to as digital signals), the discrete Fourier transform (DFT) of a sampled sinusoid is only able to represent the sinusoid's frequency perfectly if the frequency of the sinusoid is one of the discrete set of frequencies of the underlying DFT basis signals. For such signals, the DFT is a simple pulse at the specific frequency value. In this case, the DFT exhibits the frequency of the sampled sinusoid perfectly.

With the usual definition of the DFT of vector x with components x_k for $k = 0, 1, \ldots, N-1$, for some integer N, given by $X_n = \sum_{k=0}^{N-1} x_k e^{-2\pi i n k/N}$ for $n = 0, 1, \ldots, N-1$, the discrete functions $\exp(-2\pi i k n/N)$ can be seen as sampled versions of $\exp(-2\pi i n t)$ with samples at $t = k/N$, for $k = 0, 1, \ldots, N-1$.

For sinusoids with a frequency outside of the relatively small set of discrete values of the DFT basis signals, the DFT of the simple sinusoid "leaks" into the surrounding frequency values. Windowing the sinusoid is a method used to combat leakage, and windowing prior to taking the DFT does result in a narrowing of the

D.H. Mugler (✉) • S. Clary
University of Akron, Akron, OH, USA
e-mail: dmugler@uakron.edu; sclary@uakron.edu

A.I. Zayed, G. Schmeisser (eds.), *New Perspectives on Approximation and Sampling Theory*, Applied and Numerical Harmonic Analysis,
DOI 10.1007/978-3-319-08801-3_16

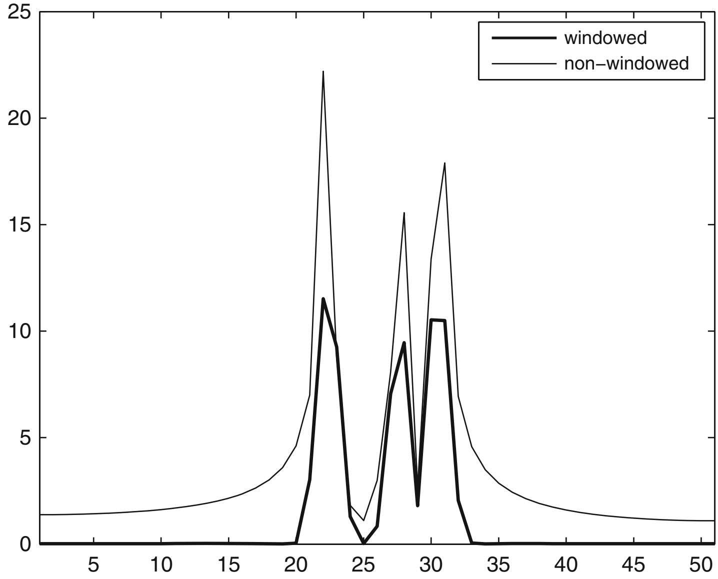

Fig. 16.1 Magnitude DFT plot of a chord of three sinusoids whose frequencies are not at a basis function frequency, and a magnitude plot of the DFT of the same chord when Gaussian-windowed

leakage, but still without enabling the determination of the specific frequency of the input sinusoid.

Consider a digital signal made up of a finite linear combination of simple sinusoids at different frequencies. We will refer to this type of an input signal as a "chord" because of the sound such a signal would create. The leakage further masks the actual frequencies, and windowing does again not completely allow for the identification of those frequencies, especially for frequencies that are relatively close to each other. See Fig. 16.1.

In this chapter, we introduce a new method to compute the frequencies in a digital signal that is based on the discrete Hermite transform (DHmT) instead of the usual DFT. The DHmT was developed by the authors in a sequence of papers, [1, 2, 9, 10]. Simply sampling the Continuous Hermite functions (CHf) over a finite discrete domain does not result in a set of vectors that retain orthogonality or any of the other of the many properties of the CHf. Defined as the eigenvectors of a specific tridiagonal matrix [1], the new set of Discrete Hermite functions (DHf) not only retain the shapes of the CHf but are also mutually orthonormal and are eigenvectors of a shifted (centered) Fourier matrix. This transform was shown to be useful in removing artifacts from EEG signals [6] and in analyzing ECG signals [5, 12]. A general overview that includes biomedical applications of the DHmT was provided in [4]. A recent paper [11] connects the DHmT to multiscale applications.

For a digital signal that is sampled values of a simple sinusoid, the DHmT has some unique properties, as will be described in Sect. 16.4, that enable the computation of the frequency of the sinusoid even when that frequency is not one of the DFT Fourier basis signals. This extends to the case of a chord where the digital signal is a finite linear combination of simple sinusoids.

Examples of applications of this new method to determine frequencies of chords are provided in Sect. 16.4. This new method provides a technique that may prove to be useful in providing additional clarity beyond the visualizations of time-frequency spectrogram plots for many digital signals. That new method is discussed and illustrated in Sect. 16.5.

16.2 Background: The Continuous Hermite Functions

The continuous Hermite functions and some of their applications are described in summary papers by Martens [7, 8]. An introduction to these classical CHf begins with Hermite polynomials, $H_n(t)$. See the overview in [4]. Interesting applications of the CHf are given in [3, 14]. Extensions to multiscale applications are given in [16] and applications of two-dimensional CHf are given in [15, 17].

The Hermite polynomials form a set of orthogonal polynomials, similar to many other sets of orthogonal polynomials. Historically, there are two slightly different ways of defining them; one form involves a monic set of polynomials, while the other form results in the leading coefficient being a power of two. The Hermite polynomials can either be defined as $H_n(t) = (-1)^n e^{t^2/2} \frac{d^n}{dt^n}\{e^{-t^2/2}\}$ for $n \geq 0$ for the monic polynomial form or as $H_n(t) = (-1)^n e^{t^2} \frac{d^n}{dt^n}\{e^{-t^2}\}$ for the case with leading coefficient being a power of two. Each of the above two forms is a rescaling of the other, so that the choice of form is not overly essential. We choose the second approach. From the second definition above, it follows that $H_0(t) = 1, H_1(t) = 2t, H_2(t) = 4t^2 - 2, \ldots$. The Hermite polynomials can be generated from a three-term recurrence relation, as is the case for other sets of classical sets of orthogonal polynomials.

More importantly, the CHf $h_n(t)$ are each defined as a normalized Gaussian multiple of the corresponding $H_n(t)$, where we are using the capital letter H to denote the Hermite polynomial and lower case letter h to denote the CHf. In particular, the CHf are defined for $n \geq 0$ by

$$h_n(t) = \frac{1}{\pi^{1/4}\sqrt{2^n n!}}\, e^{-t^2/2} H_n(t). \tag{16.1}$$

Multiplying the Hermite polynomials by a Gaussian makes the CHf so that they are essentially of finite support, although the length of that support increases as n increases. We denote the continuous Hermite transform of input function $x(t)$ by $H_m T\{x(t)\} = \int_{-\infty}^{\infty} x(t) h_m(t) dt$.

These functions satisfy many interesting relations; [13] has a chapter that includes a helpful listing of properties. For example, the CHf form an orthonormal set of functions, in the sense that $\int_{-\infty}^{\infty} h_n(t)h_m(t)dt = \delta(n-m)$, and every L^2 function has an expansion in terms of the CHf.

Most important for this chapter is that the CHf are eigenfunctions of the Fourier transform. The eigenfunction relation for CHf is

$$\int_{-\infty}^{\infty} h_m(t)e^{-2\pi i f_0 t}dt = (-i)^m h_m(f_0) \tag{16.2}$$

where $h_m(t)$ is the CHf for index m ($m \geq 0$) and f_0 is a fixed frequency.

As noted earlier, the CHf $h_m(t)$ decrease rapidly since they are all Gaussian multiples of polynomials. In particular, $h_0(t)$ is a gaussian function, so that $h_0(t)$ has no zero-crossings and is an even function. The number of zero-crossings of each CHf is given by its index, so that function $h_m(t)$ has m zero-crossings. Since the Hermite polynomials have the property that the even-indexed polynomials are even functions and the odd-indexed functions are odd functions, this is also a property of the CHf. This is a property that is shared by the DHf, and it will be important in the computational aspect of the frequency determination method described in this paper.

16.3 Background: Discrete Hermite Functions

A simple uniform sampling of the CHf, described above in Sect. 16.2, does not result in a set of vectors that retain an orthogonality property similar to that of the CHf. Further, a simple uniform sampling of the CHf does not produce vectors with an eigenvector property similar to Eq. (16.2). In contrast, defined by the authors [1] as the eigenvectors of a specific tridiagonal matrix, the set of DHf not only retain the shapes of the CHf but are also mutually orthonormal and are eigenvectors of a shifted (more precisely-centered) Fourier matrix. We call them DHf only for an analogy with the CHf, as the DHf are actually vectors.

The DHf also share other properties with the CHf. The initial function $h_0[n]$ has the shape of a Gaussian. In actuality, the lower-indexed DHf are very close to sampled versions of the corresponding CHf. The DHf vectors share the property with the CHf that even-indexed functions are even functions, and odd-indexed functions are odd functions. Those properties are easily visible in the plots of some of the even-indexed DHf together with some of the odd-indexed DHf in Fig. 16.2.

Important for this chapter is that the DHf are eigenvectors of the centered Fourier matrix. In particular,

$$\mathcal{F}_{\mathcal{C}} \cdot h_k = (-i)^k h_k, \tag{16.3}$$

where the left side of Eq. (16.3) is matrix-vector multiplication with $\mathcal{F}_{\mathcal{C}}$ as the centered Fourier matrix analogous to the usual continuous Fourier transform and

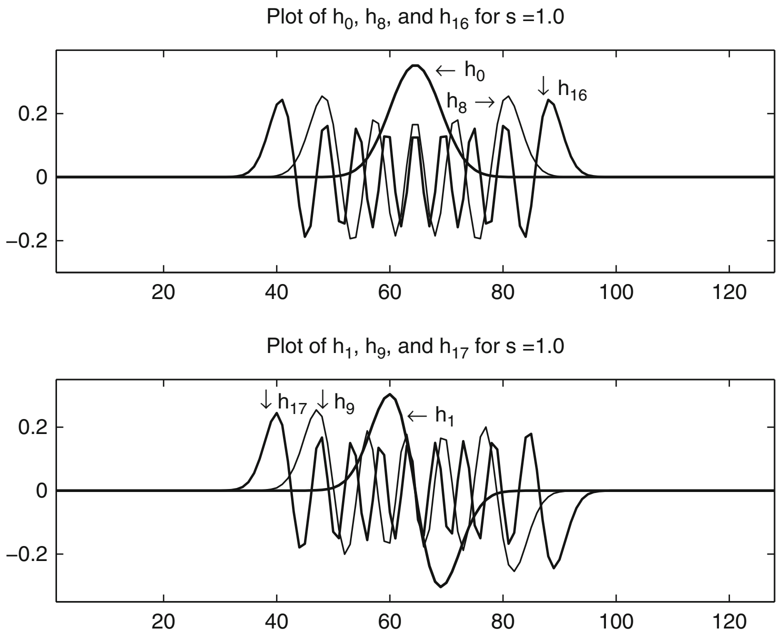

Fig. 16.2 Plots of several of the even-indexed (*top*) and odd-indexed (*bottom*) discrete Hermite functions

with h_k as the kth eigenvector, $k \geq 0$. Note that Eq. (16.3) is a discrete analog of Eq. (16.2).

As explained in [1], the DHf are eigenvectors of a symmetric tridiagonal matrix, so they form an orthonormal set of eigenvectors, and every vector of length N can be expressed as a linear combination of the DHf. Since the DHf are produced as eigenvectors of a very sparse matrix, it is also a fast computational process to produce the entire set of DHf, even for very large lengths N.

16.4 The Discrete Hermite Transform of a Sampled Sinusoid

The continuous Hermite transform of a sinusoid, $H_mT\{\sin(2\pi f_0 t)\}$, can be simplified using the eigenfunction relation (16.2) of the CHf for the continuous Fourier transform. For fixed frequency f_0 and index n, the continuous Hermite transform value is given by

$$\begin{aligned} \int_{-\infty}^{\infty} h_n(t)\sin(2\pi f_0 t)\, dt &= \int_{-\infty}^{\infty} h_n(t)(e^{2\pi i f_0 t} - e^{-2\pi i f_0 t})/2i\ dt \\ &= (-i)^{n-1}(h_n(-f_0) - h_n(f_0))/2i \end{aligned} \tag{16.4}$$

But a well-known relation described in Sect. 16.2 for the CHf is that h_n is an even function if n is even and an odd function if n is odd. Using those relations in the second part of Eq. (16.4), the Hermite transform of the sinusoid becomes zero if n is even, and $(-1)^{(n-1)/2}h_n(f_0)$ if n is odd. That is, the continuous Hermite transform of the sinusoid is zero for even indices and equals $(-1)^k h_n(f_0)$ when $n = 2k + 1$ is odd.

Using a similar argument, the Hermite transform of $\cos(2\pi f_0 t)$ is zero for odd indices and equals $(-1)^{n/2}h_n(f_0)$ when the index is even.

These formulas can be combined to give an expression valid for the Hermite transform of a sinusoid shifted with arbitrary phase angle. Suppose that the general sinusoidal input signal includes a phase angle ϕ as $x(t) = \sin(2\pi f_0 t + \phi)$. Then the standard sinusoidal identity $\sin(2\pi f_0 t + \phi) = \cos\phi \sin(2\pi f_0 t) + \sin\phi \cos(2\pi f_0 t)$ leads to a general expansion for the Hermite transform of the general sinusoid as

$$H_m T\{\sin(2\pi f_0 t + \phi)\}(n) = \begin{cases} \sin\phi \cdot (-1)^{n/2} h_n(f_0) & \text{if } n \text{ is even} \\ \cos\phi \cdot (-1)^{(n-1)/2} h_n(f_0) & \text{if } n \text{ is odd} \end{cases} \tag{16.5}$$

Equation (16.5) is the key equation that will be extended to a discrete analog.

Besides having specific formulas for the continuous Hermite transform of a general sinusoid, note that the angle ϕ can be approximately recovered from successive values of the transform. This is because successive values of the transform values include $\sin\phi$ and $\cos\phi$ as corresponding multiples. To recover the phase angle, start by taking the ratio of the values of $HmT\{\sin(2\pi f_0 t + \phi)\}(m)$ for $m = n$ and $m = n + 1$, for n even.

16.4.1 The Hermite Matrix H

There is a discrete analog of the general formula for the continuous Hermite transform of a sinusoid, as was given in Eq. (16.5) above.

The Hermite matrix H is defined to be the matrix of size $N \times N$ with columns $h_0, h_1, \ldots, h_{N-1}$. With this definition of H, the DH_mT of input vector x is the matrix-vector product $H' \cdot x$, with the prime indicating transpose.

As an example of matrix H, Table 16.1 is the complete set of values of the first three columns of H for the 8×8 case, displayed in transpose form. Note how each column in the top half of the matrix is reflected as either an even or an odd vector over the bottom half of the matrix. It is important for the following to note that the general case of the H matrix has this vertical symmetry about the middle rows, up to minus signs. It is the even/odd symmetry of the DHf that makes it so that matrix H has symmetry about the horizontal between rows $N/2$ and $N/2 + 1$ in the table.

Table 16.1 The values of the first three columns of the Hermite matrix H for the 8×8 case listed in transpose form

$H(:, 1:3)' =$

0.0025	0.0549	0.2962	0.6397	0.6397	0.2962	0.0549	0.0025
0.0131	0.1844	0.5593	0.3911	−0.3911	−0.5593	−0.1844	−0.0131
0.0463	0.3885	0.5210	−0.2748	−0.2748	0.5210	0.3885	0.0463

16.4.2 Frequency Computation Using the DHmT of a Sampled General Sinusoid

Suppose that the general sinusoid $gsx(t) = \sin(2\pi f_0 t + \phi)$ is sampled uniformly with sample spacing $T = 1/N$ and that the sampling vector is centered. That is, the N samples of the sinusoid are specified at sample points starting with the vector $t = -(N-1)/2, \ldots, (N-1)/2$ which is then normalized by dividing by $\sqrt{N}$. In order to provide a discrete analog to Eq. (16.5) exactly, f_0 in the following needs to be one of the discrete set of frequencies $p + \frac{1}{2}$ for $p = 0, \ldots, N/2 - 1$. With f_0 as an integer plus one-half, then $p = f_0 - 1/2$. The Nyquist criterion for digital signals results in a limit on the frequencies f_0 that are allowed for sampling without aliasing. In particular, $f_0 \le N/2$ for the uniform sampling described above.

For the general sinusoid, suppose that the vector is sampled as described above from a general sinusoid gsx. The DHmT of the discretized general digital input sinusoid can be shown to be given by

$$DH_mT\{gsx(f_0)\}[k] = \begin{cases} \sin\phi \cdot (-1)^q h_k[p] & \text{with } q = k/2 \text{ when } k \text{ is even} \\ \cos\phi \cdot (-1)^q h_k[p] & \text{with if } q = (k-1)/2 \text{ when } k \text{ is odd} \end{cases} \tag{16.6}$$

for $0 \le k \le N-1$, where $f_0 = p + \frac{1}{2}$. Note the similarity of this result to Eq. (16.5).

In terms of the Hermite matrix H as described in Sect. 16.4.1, Eq. (16.6) means that the DHmT transform of a sinusoid sampled as described above comes from the *values of a corresponding* ***row*** *of matrix H.* In the case of a sinusoid with phase $\phi = 0$, every other value of the transform is equal to zero and some values are multiplied by -1. As an example to illustrate (16.6), for a general sinusoid with $\phi = 0$ and frequency $f_0 = 2.5$, it is the third row after the middle row of the H matrix that gives the corresponding values. Note that every other entry of the DHmT has exactly the same magnitude as the entry of the referenced row of the H matrix (Table 16.2).

The Hermite matrix H described in Sect. 16.4.1 contains the DHf as column vectors. As a set of eigenvectors of a symmetric matrix, this set of vectors is mutually orthogonal. H is an orthogonal matrix, and the rows are also mutually orthogonal. Since the DHmT of a uniformly sampled general sinusoid is closely related to one of the rows in this matrix, we can determine the location of that row using orthogonality between rows. Since the frequency of the sinusoid is related to the row location, we can use this to determine the frequency of the sinusoid.

Table 16.2 To illustrate Eq. (16.6)

k:	0	1	2	3	4	5	6	7	8	9
DHmT(sx):	0	0.4207	0	−0.1508	0	−0.3276	0	−0.2687	0	−0.1237
H row 13:	0.2116	0.4207	0.4371	0.1508	−0.2293	−0.3276	−0.0434	0.2687	0.2115	−0.1237

These two sets of paired vector values provide the first ten entries of the DHmT of a centered sinusoid with $N = 20$, $f_0 = 2.5$, and $\phi = 0$. The top row is the first ten values of the DHmT for $k = 0, \ldots, 9$ along with the corresponding entry of row 13 of matrix H listed below it

To eliminate the redundancy that is in matrix H, we use the bottom half only of this matrix in the following. In particular, first form the rectangular matrix of size $N/2 \times N$ that includes rows $N/2+1$ to N of the square Hermite matrix H. Finally, change the sign on every other even-indexed column and on every other odd-indexed column. The result is called H_ϕ in the following. Note that H_ϕ retains the property of having row orthogonality.

The rectangular matrix H_ϕ is used to determine the location of the row that is related to the DHmT of the sinusoid. In particular, compute the matrix-vector product,

$$\hat{x} = H_\phi \cdot DHmT(x), \tag{16.7}$$

so as to use the orthogonality between rows. Note that we label the resulting vector above as $\hat{x}$, as something of a transform itself of the sampled input sinusoid. It is from a slight modification from $\hat{x}$ that we will obtain a highly accurate estimate of the frequency and amplitude of the sinusoid.

In particular, construct the modified vector $\hat{x}_m$ with components defined by summing odd-indexed and even-indexed entries of $\hat{x}$,

$$\hat{x}_m[k] = 2(\hat{x}[2k-1] + \hat{x}[2k]), \tag{16.8}$$

for $k = 1, \ldots, N/2$. This vector can be useful, particularly if the phase angle ϕ of the input sinusoid is desired. However, it is generally the frequency and amplitude of the input sinusoid that are most desired. For that, construct the following squared and combination version of $\hat{x}$ that eliminates the dependence on the phase angle of the input sinusoid: Define F_m by

$$F_m[k] = 4(\hat{x}[2k-1]^2 + \hat{x}[2k]^2) \tag{16.9}$$

for $k = 1, \ldots, N/2$.

For example, define input function x as the sum of two sinusoids:

$$x = 10.24 \sin(2\pi(10.95)t) + 10.8 \sin(2\pi(25.05)t + \pi/3) \tag{16.10}$$

and suppose that this is sampled uniformly with $N = 100$ and then normalized by $\sqrt{N}$ as described above. For this example, the corresponding $\hat{x}_m$ and F_m vectors are as plotted in Fig. 16.3. Note the pulse-like shapes close to the locations of the two sinusoidal frequencies at 10.95 Hz and 25.05 Hz of the input signal.

It is important to note that if the frequency of the input sinusoid has the form of integer plus 0.5, then each of the above vectors is simply a pulse at the corresponding frequency integer. This follows from the formation of rectangular matrix H_ϕ as one of the rows in the DHmT of a sinusoid. This is the easiest case for determining the frequency.

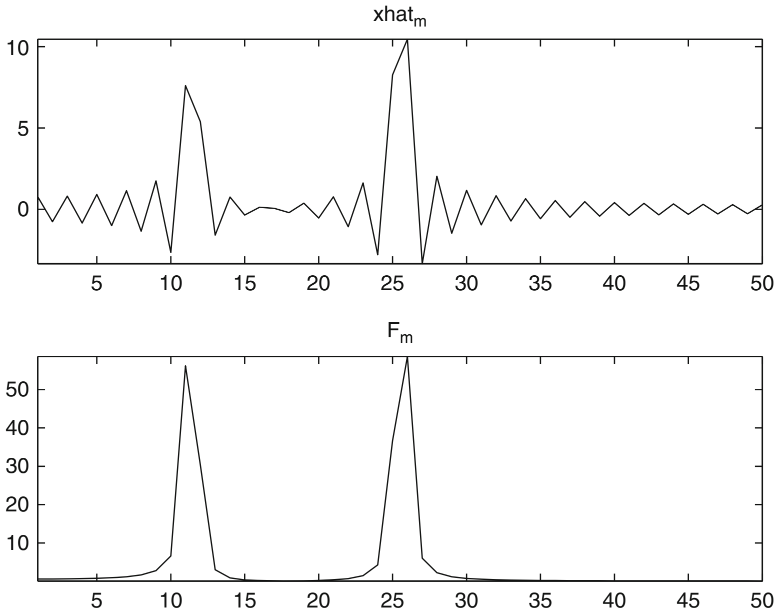

Fig. 16.3 The Hermite evaluation vectors for the example input sinusoid (16.10). $\hat{x}_m$ is in *top* plot and F_m is on the *bottom*

16.4.3 Sinc Model for Frequency Determination

The top plot of $\hat{x}_m$ in Fig. 16.3 has the general appearance of a sum of sampled sinc functions combined linearly. This general form provides a very good approximation of the $\hat{x}_m$ vector, and a linear combination of squared sinc functions is also a very good approximation to the F_m vector. These approximations can be used to provide highly accurate estimates of both the frequencies and amplitudes of an input that is a linear combination of sampled sinusoids.

Suppose that input function $x(t)$ is a linear combination of sinusoids, so that x is a chord as described previously, of the form $x(t) = \sum_{k=1}^{n} a_k \sin(2\pi f_k t + \phi_k)$, where the amplitudes, frequencies, and phases of the individual sinusoids are given by the vectors a, f, and ϕ, respectively.

The sinc model to approximate $\hat{x}_m$ for a sampled linear combination of sinusoids as defined above is given by

$$\hat{x}_m \approx \sum_{k=1}^{n} a_k (\cos(\phi_k) + \sin(\phi_k)) \operatorname{sinc}(t - f_k). \tag{16.11}$$

Note that this depends on the phase angle ϕ, which is not a value as desirable to be determined as are frequency and amplitude. In Eq. (16.11), $\hat{x}_m$ on the left is a vector and the approximation in Eq. (16.11) assumes sampling of the sinc function.

The sinc model to approximate the value F_m, as in Eq. (16.9), for a sampled linear combination of sinusoids as defined above is given by

$$F_m \approx \sum_{k=1}^{n} a_k^2 \, \mathrm{sinc}^2(t - f_k) \tag{16.12}$$

In summary, the following is a listing of the computational procedure for estimating frequencies and amplitudes of a linear combination of uniformly sampled sinusoids: Compute the DHmT of the input; compute the product of the modified Hermite matrix and the DHmT of x by $\hat{x} = H_\phi \cdot DHmT(x)$ as given in Eq. (16.7); form the vector F_m as given in Eq. (16.9); determine the number of peaks and their locations in the vector F_m (use the number of peaks as an estimate of the number of sinusoids in the input signal); fit a single shifted sinc-squared function from Eq. (16.12) to F_m in the vicinity of each peak.

For each peak, the least-squares fit of Fm to the squared and shifted sinc function will provide the estimate of the correct amplitude a_k and frequency f_k. Subtract the result from F_m, thereby removing the peak at that location. Repeat the function fitting in the vicinity of the next peak for the estimate of the next amplitude and frequency. Continue this process until all frequencies f_k and amplitudes a_k have been estimated. The accuracy of estimating frequencies and amplitudes of the input signal is tied to the ability of the least-squares fitting method to estimate those values, as outlined in the last step of the procedure listed above.

As an example, suppose that the input function is the linear combination of two sinusoids as given in the example in Sect. 16.4.2 by Eq. (16.10). Using the procedure outlined above, estimates for frequencies and amplitudes give results as follows: The two frequencies of 10.95 and 25.05 Hz are estimated as 10.924 and 25.059 Hz, resp. The corresponding amplitudes of 10.24 and 10.8 are estimated as 10.289 and 10.797, resp.

16.5 The HDgram: A New Method for Time-Frequency Representations

Images given by spectrograms, which use Fourier analysis, and by scalograms, which use wavelets, are established methods for time-frequency representations. Frequency characterization by the discrete Hermite transform provides a new method for creating time-frequency images that can be more focused, particularly for input signals that are a linear combination of sinusoids. We call such a time-frequency image an HDgram, interpreted as Hermite distribution for frequencies and amplitudes over time.

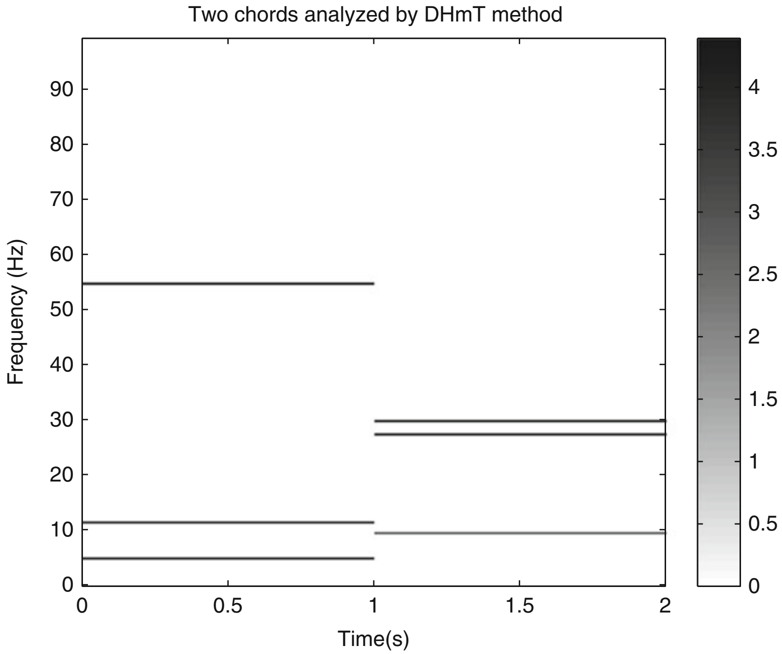

Fig. 16.4 The HDgram time-frequency plot of the two chords described in the text, each consisting of three sinusoids at distinct frequencies

The technique for creating an HDgram is the same as for a spectrogram, except that the DHmT is applied instead of an FFT and the procedure for frequency analysis used is that outlined in Sect. 16.4.3 above.

As an example, we consider an example of an HDgram of a fairly simple signal that consists of two chords of three frequencies that change once over the time interval of interest. For this example, the chord over the first half of the time interval consists of sinusoids with frequencies of 5.45, 12.1, and 55.7 Hz with corresponding amplitudes of 10.2, 8.8, and 16.75, resp. The chord over the second half of the time interval consists of sinusoids with frequencies of 9.85, 28.08, and 30.5 Hz with corresponding amplitudes of 4.24, 19.8, and 10.75, resp.

The HDgram of these two simple chords is displayed in Fig. 16.4. The HDgram shows each of these frequencies very accurately with little distortion at the beginning and end of the time interval of transition. The darkness or coloring of the lines at particular frequencies is tied to the logarithm of the amplitudes of the sinusoids in each case. Overlapping was not used in creating this HDgram. Note how clearly the three different frequencies in each time interval are illustrated, and also how clearly the frequencies that are relatively close to each other in the second interval are differentiated from each other. In this case, frequencies are in error by no more than 0.7 % with an average error of 0.3 %, and the amplitudes have error no more than 14.9 % with an average error of 3.8 %.

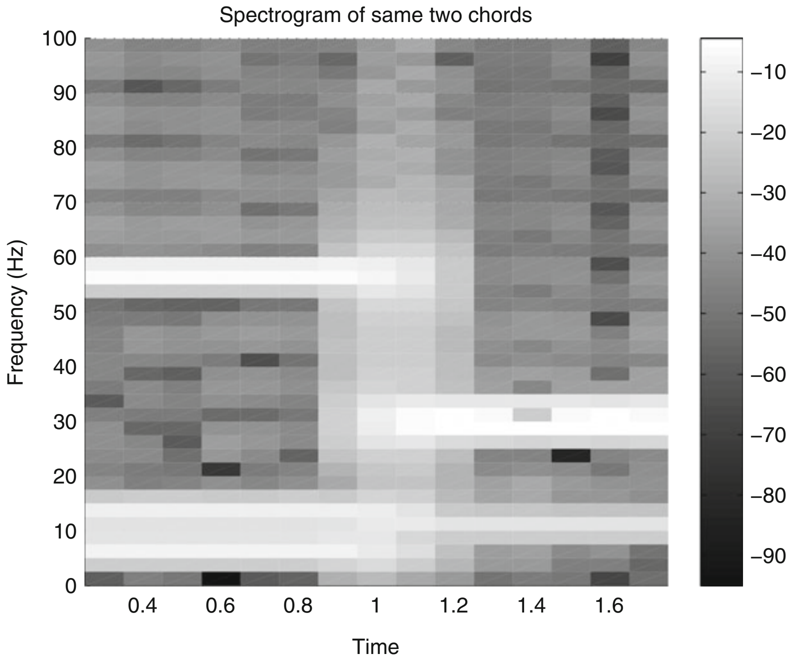

Fig. 16.5 Spectrogram of same two chords as imaged in Fig. 16.4

For comparison, given in Fig. 16.5 is the spectrogram for the same two chords with the same input vector as was used for the HDgram in Fig. 16.4. Note how the beginning and ending of the sinusoids over the two intervals are smeared and difficult to determine with any accuracy. Also note that the two frequencies near 30 Hz in the second half of the interval are not clearly differentiated and appear as one frequency. The additional colorings in the spectrogram, such as the many darker rectangles, are artifacts in the spectrogram and do not represent any real frequencies present in the signal. This spectrogram was created for an input of $N = 200$ digital samples using an overlap of 80.

16.6 Conclusions

This chapter has introduced a new way of determining frequency and amplitude content of a signal based on the DHmT. The DHmT has been introduced by the authors in a sequence of papers. The accuracy of the frequency determination in this new method helps to reduce the problem of spectral leakage, a common problem due to sampling that was discussed in Sect. 16.1.

Relations and common properties shared by the CHf and the DHf were provided in Sect. 16.4, but the most important of those properties in the analysis of frequencies and amplitudes is that of being eigenfunctions (eigenvectors) for the Fourier transform (centered Fourier matrix), resp. That property is the one that provides the general form of the continuous or DHmT of a sinusoid, as given in Eqs. (16.5) and (16.6).

For the discrete case, the DHmT of a sinusoid is a modified row of the Hermite matrix H. Since the rows in that matrix are mutually orthogonal, we can determine the row number, and thereby the frequency, using inner products of what is equivalent to the other rows in that matrix. Simplifying that square matrix to rectangular matrix H_ϕ in Sect. 16.4 provided a computational method for both frequencies and amplitudes, as given in Sect. 16.4.3.

This method is appropriate to evaluate frequencies of input functions that are not at a basis function frequency. For frequencies that are at an integer plus 0.5, the evaluation vector F_m is a pulse, but for other frequencies, the sinc model provides a means to form a highly accurate estimate of both frequencies and amplitudes, as prescribed in Sect. 16.4.3.

Applying this method to an input signal that is a linear combination of sinusoids that can change over a time interval was shown in Sect. 16.5 to provide a new time-frequency image called the HDgram. An example of an input signal that is of chords changing over time showed the ability of the HDgram to provide more clarity and definition to time-frequency images than spectrograms for this case. This new method may prove to be useful in providing additional clarity in the visualization of time-frequency images for many digital signals.

Acknowledgments The authors are grateful to Jacob Trombetta, master's student of the first-named author, for some initial development.

References

1. Clary, S., Mugler, D.H.: Shifted Fourier matrices and their tridiagonal commutors. SIAM J. Matrix Anal. **24**(3), 809–821 (2003)
2. Clary, S., Mugler, D.H.: Eigenvectors for a class of discrete cosine and sine transforms. Sampl. Theory Signal Image Process. **3**, 83–94, (2004)
3. Escalante-Ramrez, B., Martens, J.B.: Noise reduction in computerized tomography images by means of polynomial transforms. J. Visual Comm. Image Rep. **3**, 272–285 (1992)
4. Gopalikrishnan, R., Mugler, D.H.: The evolution of Hermite transform in biomedical applications. In: Shukla, A., Tiwari, R. (eds.) Intelligent Medical Technologies and Biomedical Engineering: Tools and Applications, pp. 260–278. IGI Global, Hershey (2010)
5. Gopalikrishnan, R., Acharya, S., Mugler, D.H.: Real time monitoring of ischemic changes in electrocardiograms using discrete Hermite functions. In: Proceedings of 26th International Conference of the IEEE, Engineering in Medicine and Biology Society, pp. 438–441. IEEE, Piscataway, New Jersey (2004)
6. Mahadevan, A., Acharya, S., Sheffer, D., Mugler, D.H.: Ballistocardiogram artifact removal in EEG-fMRI signals using Discrete Hermite transforms. IEEE J. Sel. Top. Signal Process. (Special Issue on: fMRI Analysis for Human Brain Mapping) **2**(6), 839–853 (2008)

7. Martens, J.B.: The Hermite transform-theory. IEEE Trans. Acoust. Speech Signal Process. **38**(9), 1595–1606 (1990)
8. Martens, J.B.: The Hermite transform-applications. IEEE Trans. Acoust. Speech Signal Process. **38**(9), 1607–1618 (1990)
9. Mugler, D.H., Clary, S.: Discrete Hermite functions. In: Proceedings of the International Conference on Scientific Computing and Mathematical Modeling, IMACS 2000, pp. 318–321. Milwankee, Wisconsin (2000)
10. Mugler, D.H., Clary, S.: Discrete Hermite functions and the fractional Fourier transform. In: Proceedings of the International Workshop on Sampling Theory, pp. 303–308. IEEE, Piscataway, New Jersey (2001)
11. Mugler, D.H., Mahadevan, A.: Multiscale signal processing with discrete Hermite functions. In: Shen, X., Zayed, A.I. (eds.) Multiscale Signal Analysis and Modeling, pp. 257–274. Springer, New York (2012)
12. Mugler, D.H., Clary S., Wu, Y.: Discrete Hermite expansion of digital signals: applications to ECG signals. In: Proceedings of the IEEE Signal Processing Society 10th DSP Workshop, pp. 271–276. Georgia (2002)
13. Poularikas, A.D.: The Handbook of Formulas and Tables for Signal Processing. CRC Press, Boca Raton (1999)
14. Refregier, A.: Shapelets I. A method for image analysis. Mon. Not. R. Astron. Soc. **338**, 35–47 (2003)
15. Rodieck, R.W.: Quantitative Analysis of cat retinal ganglion cell response to visual stimuli. Vision Res. **5**, 583–601 (1965)
16. Silván-Cárdenas, J.L., Escalante-Ramrez, B.: The multiscale Hermite transform for local orientation analysis. IEEE Trans. Image Process. **15**, 1236–1253 (2006)
17. Van Rullen, R., Thorpe, S.J.: Rate coding versus temporal order coding: what the retinal ganglion cells tell the visual cortex. Neural Comput. **13**, 1255–1283 (2001)